Research Article | Vol. 31, No. 23 / 6 Nov 2023 / Optics Express 39030
Optics EXPRESS

Narrow linewidth and wideband tunable continuous-wave terahertz generator based on difference frequency generation with DAST crystal

ZELONG WANG,[1,2] YUYE WANG,[1,2,*] HAIBIN LI,[1,2] MEILAN GE,[1,2] DEGANG XU,[1,2] AND JIANQUAN YAO[1,2]

[1] School of Precision Instruments and Optoelectronics Engineering, Tianjin University, Tianjin 300072, China
[2] Key Laboratory of Optoelectronic Information Technology (Ministry of Education), Tianjin University, Tianjin 300072, China
[*] yuyewang@tju.edu.cn

Abstract: A narrow linewidth and wideband tunable continuous-wave terahertz generator with DAST crystal has been demonstrated in this paper. Two narrow-linewidth CW fiber lasers were used as the pump sources for difference frequency generation. The terahertz wave can be continuously tunable in the range of 1.1-3 THz. The maximum output power of 2.79nW was obtained at 2.568 THz. The linewidth of the output THz wave was estimated to be 56.5 MHz by fitting transmission spectrum of CO gas at 450 Pa pressure around 80.52 cm^{-1} with the Vogit gas model. Furthermore, the output spectra at room temperature and pressure was in good agreement with the air absorption lines in Hitran database. Moreover, the narrower absorption characteristic spectrum of 2-Deoxy-D-Glucose sample has been obtained through the spectrum measurements. Therefore, it could promote the practical prospect of tunable CW-THz source, which will have good potential in THz high-precision spectroscopic detection and multispectral imaging.

1. Introduction

Terahertz (THz) spectral range is located between the infrared (IR) and the microwave bands, which plays a vital role in practical applications, such as biological imaging, environmental monitoring, non-destructive evaluation, spectroscopy and molecular analysis [1–6]. To reveal the intramolecular vibration/rotation information of various compounds, of which the linewidth of absorption lines typically in GHz or even MHz range [7], THz wave with wide tunability, narrow-linewidth, high frequency accuracy as well as high power stability is required.

There are a number of methods to generate THz wave, including solid-state frequency multiplier technology [8], electron cyclotron resonance maser [9], free electron laser (FEL) [10], quantum cascade laser (QCL) [11], gas pumped THz laser [12], ultrashort pulse pumped terahertz-wave generation [13], and nonlinear optical frequency conversion [14,15]. The solid-state frequency multiplier technology can generate THz wave with MHz level linewidth. However, the frequency is normally below 1 THz and the tunable range is about several GHz due to the limit of the diode performance. Electron cyclotron resonance maser has high output power and efficiency. Limited by the structure characteristics, it is difficult to generated tunable high frequency THz wave. FEL is an effective method to obtain high power THz radiation with wide tuning range, but the high manufacturing and usage costs make it difficult to be widely applied for research. QCL can realize high-power and narrow linewidth THz wave output. However, the THz tuning gap is relative narrower. The processing of multilayer CMOS chips and the low-temperature system operation still require further research. Although gas pumped THz laser has narrow linewidth and high output power, frequency tuning is realized by replacing pump gas, which

#506367 https://doi.org/10.1364/OE.506367
Journal © 2023 Received 21 Sep 2023; revised 18 Oct 2023; accepted 23 Oct 2023; published 1 Nov 2023

Optics EXPRESS

is inconvenience for spectroscopy research. Terahertz time-domain spectrometer (THz-TDS) based on ultrashort pulses is the most widely used source for THz spectroscopy detection. Currently, the linewidth with GHz level and low SNR at higher frequency still restrict its further applications in reveal intramolecular information. THz difference frequency generation (DFG) sources based on nonlinear optical frequency conversion is a promising method to generate wide tunable, narrow-linewidth THz wave [16,17]. Here, nonlinear crystals including inorganic and organic crystals play the key role in nonlinear process. For inorganic crystal, uneven refractive characteristics lead to a narrow tuning range and usually requires complex crystal angle tuning devices [15,18]. For organic crystal, such as DAST, DSTMS, OH1, it has the advantage of high nonlinear coefficients and can easily meet the phase matching conditions for IR and THz range due to the flat refractive characteristics [19,20]. Thus, continuously tuned THz wave output can be obtained over a large tuning range by simply adjusting the pumping wavelength [21]. Moreover, considering that the linewidth of THz wave is related to the linewidth of the dual-wavelength pump light in DFG, continuous-wave (CW) laser with narrower linewidth is more suitable to be pumping source compared with the pulsed laser [22,23]. Until now, dual-wavelength laser based on VECSEL laser and fiber laser has been used for the pump source of CW-DFG [17,23,24], the tuning range of these methods was narrow, making it difficult to generate a wide band tuning THz wave.

In this paper, a narrow linewidth and tunable CW-THz source with DAST crystal via DFG has been presented in this work. A narrow linewidth pump light with a fixed wavelength of 1536.8489 nm and another narrow linewidth pump light with a tuning range from 1545 nm to 1561 nm were used as a dual-wavelength pump light. The continuous tunable THz frequency range was realized from 1.1 THz to 3 THz using DAST crystal. The maximum output power of 2.79 nW was obtained at 2.568 THz. The power fluctuation in 30 minutes was measured to be 2.41%. Furthermore, the linewidth of the THz wave was estimated to be 56.5 MHz through CO gas detection. The THz output spectra in 20°C and 40% humidity consisted well with the air absorption lines in Hitran database, indicating the THz source has high spectral accuracy. In addition, the narrower absorption characteristic spectrum of 2-Deoxy-D-Glucose sample has been obtained through the spectrum measurements. Such kind of THz source would have good potential in THz high-precision spectroscopic detection and multispectral imaging.

2. Experimental setup

Figure 1 shows the schematic diagram of the CW-THz source based on DFG with DAST crystal. In this experiment, two CW fiber lasers and one amplifier provided the dual-wavelength pump lights. Laser1 (T100S-HP, EXFO Inc.) can generate a ~mW narrow linewidth polarized light in the range of 1500-1630 nm, which was then boosted to higher power in the range of 1545-1561 nm by an amplifier (KEOPSYS CEFA-C-PB-HP, Lumibird Inc.). Laser2 (CoSF-D-ER-B-MP, Connet Fiber Optics Co. Ltd.) can generate a high power, narrow linewidth CW light at a fixed wavelength of 1536.8489 nm. The output wavelengths of both lasers were precisely measured using a wavelength meter (AQ6151, Yokogawa Co. Ltd.) to ensure the frequency accuracy of the generated THz waves. The half-wave plates (HWP1 and HWP2) were used to adjust the polarization of two pump lasers, respectively. The collimating systems (L1 and L2, L3 and L4) were used to adjust two pump beams to have almost the same beam waist and divergence angles. M1 ($R \geq 99\%$ at 1400-1600 nm) and M2 ($T \approx 75\%$ at 1545-1561 nm and $R \approx 75\%$ at 1536.8489 nm) were used to combine two laser beams into one line. The collimation and the alignment were observed with a beam analyzer to realize high overlap of the dual-wavelength beam, which can ensure high power conversion efficiency during nonlinear frequency conversion. Then, dual-wavelength beam was focused by an objective lens (L5) with a beam waist diameter of 40 μm. A DAST crystal (Rainbow Photonics Ltd.) without coating was placed at the focal point to achieve collinear phase-matched DFG to generate THz wave. The size of DAST crystal

Optics EXPRESS

was 3 mm in diameter and 570 ± 20 µm in thickness, the dual-wavelength beam propagates along *c*-axis of DAST with *a*-axis polarization. After that, an off-axis parabolic mirror (OAP1) with 2.5 mm hole aperture was used to collimate and separate the generated THz wave and residual pump. OAP2 was used to focus and inject THz wave into a 4K-Bolometer (IR-labs Inc.) for power detection. Dump1 and Dump2 were used to absorb the residual NIR light. Considering the response rate of 4K-Bolometer, an optical chopper (Stanford Research Systems, SR540) with a certain chopping frequency was placed before DAST crystal, which also can reduce the thermal damage for organic crystal. A piece of black polyethylene (PE) with the thickness of 0.6 mm was inserted before the detection window of 4K-Bolometer to filter out the residual NIR signal and stray light.

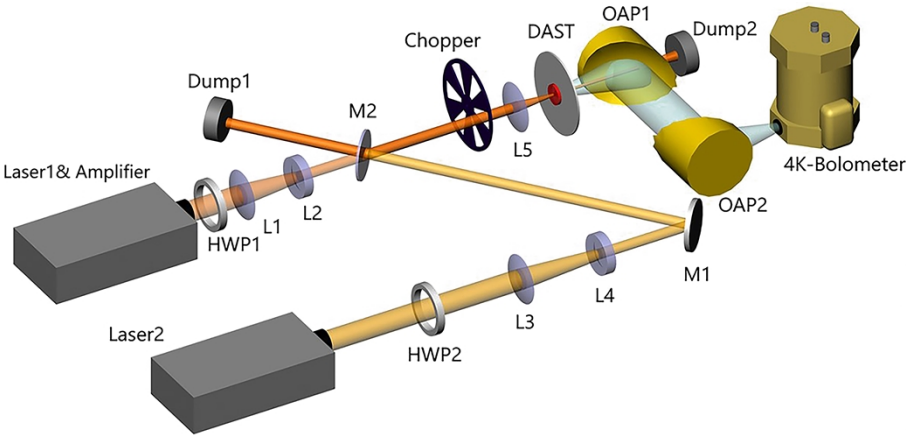

Fig. 1. Schematic diagram of the CW-THz difference frequency generation.

3. Results

Considering the absorption of THz waves by water vapor, the dried air was blow into the THz generation and detection parts to reduce the humidity to less than 3% in our experiment. Figure 2(a) shows the measured frequency tuning range and corresponded THz output power under the dual-wavelength pump power of 3 W, where the ratio of the power of two wavelengths was 1:1. The tunable characteristic was measured in 124 MHz/step. A chopper with the frequency of 100 Hz and the duty cycle of 1:1 was used. With the tunable IR wavelength varying from 1545 nm to 1561 nm, continuously tunable THz output from 1.1 THz to 3 THz was achieved. Based on the responsivity of Bolometer and the transmission of the black PE measured by THz-TDS, the CW THz output power can be obtained. Due to the resonance of the transverse optical phonon around 1.1 THz in DAST crystal [25], the THz power in the range of 1.1 THz to 1.4 THz was relatively low. Comparatively, ~nW-scale output was achieved in the 1.4-3 THz range. The maximum power of 2.79 nW was obtained at 2.568 THz, corresponding to the power conversion efficiency of 0.93×10^{-9}. The decay of the THz output power and damage on the crystal have not been observed after 1 hour of laser illumination at the pump power of 3 W. To avoid possible damage to the crystals, the crystal was not illumination in higher power. The black line in Fig. 2(a) was the fitting curve of the THz tuning output spectrum. It can be seen that there still were some dips in the fitting curve, which was due to the strong absorption of water vapor even at very low humidity. Especially, it is worth mentioning that THz tuning range can be furtherly expanded by increasing the tuning range of Laser1 and the related amplifier. To evaluate the stability of CW-THz source, the THz signal intensity in 30 min at 2.568 THz were measured, as shown in Fig. 2(b), where the inset shows the detected THz signal from Bolometer. The power

Optics EXPRESS

fluctuation was measured to be 2.41% in 30 min. Due to the high power stability of CW pump lasers, the output intensity of THz wave had a relative high stability, which is favorable for THz spectroscopic application.

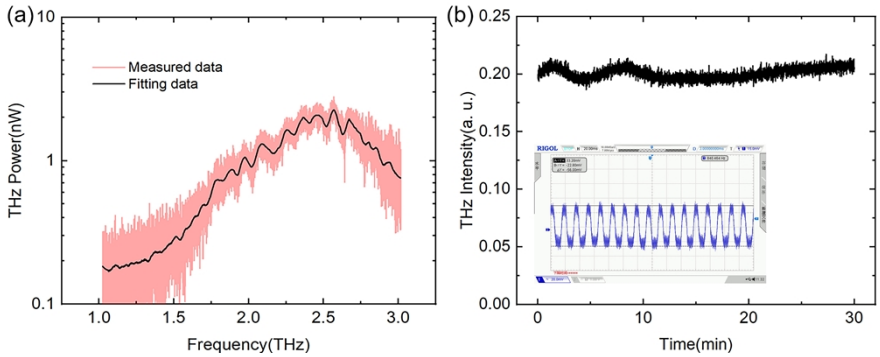

Fig. 2. (a) Tunable characteristics of CW-THz source. (b) Stability of the generated THz power over a time frame of 30 min at 2.568THz.

Due to the lower thermal damage threshold of organic crystal, higher CW power pumping may cause severe damage to the crystal. According to Ref. [26], the thermal dissipation time of organic crystal is about ~ms-scale, the heat accumulation of crystals can be effectively weakened by shortening the pumping time and increasing the pumping interval. Considering both the response rate of 4K-Bolometer and thermal dissipation of DAST crystal, the chopper frequency of 15 Hz with the duty cycle of 1:59 was set to investigate the THz output power characteristic, where the pumping duration within each cycle was 1.11 ms. Figure 3(a) shows the detected THz intensity of the Bolometer as a function of the dual-wavelength pump power at 1.684 THz, 1.986 THz and 2.568 THz, respectively, where the ratio of the pump power of two wavelengths was 1:1. As can be seen from the figure, the THz wave intensity was increased with the increase of the pump power. The higher pump power was, the higher THz wave intensity can be obtained. When the dual-wavelength pump power was improved to 10 W, the intensity of THz wave could reach about 4 times of that at 3 W pumping. It should be noted that saturation of the DFG process was not observed, implying that further boosting of the pump power can generate a higher output power of THz wave. Moreover, the polarization characteristics of the THz wave was measured using a wire grid polarizer (Microtech Instruments, Inc.), as shown in Fig. 3(b). Based on the measurement results, it can be seen that the THz wave has a high polarization extinction ratio of 9.37 dB. The better linear polarization characteristics are more suitable to the use of THz sources for some polarization-sensitive sample detection.

For THz source, beam quality is an important character in many research fields such as environmental monitoring, biological imaging, spectroscopy detection, and so on. Firstly, the beam qualities of both pump beams were measured using the near-infrared beam analyzer. The M^2 of both pump beams were less than 1.05, and the ellipticity were greater than 98%. Then, the generated THz beam waist and divergence angle were measured using knife-edge method. Figure 4(a) and (b) show the spatial distribution of the THz wave in the horizontal and vertical directions, respectively. It can be seen that the THz beam had a good Gaussian distribution in both directions. The beam waist was 6.75 mm × 7.80 mm in the horizontal and vertical directions, respectively. The divergence angle of the THz wave was 22.6 mrad ×26.3 mrad in horizontal and vertical directions, respectively. Correspondingly, the M^2 of THz beam was 2.05 and 2.76 in horizontal and vertical directions respectively, where the beam ellipticity was 87%. Compared with the pump beams, the beam quality and the ellipticity of the THz beam were reduced, which was mainly limited by the surface flatness and internal uniformity of organic crystals. Thus, the

Optics EXPRESS

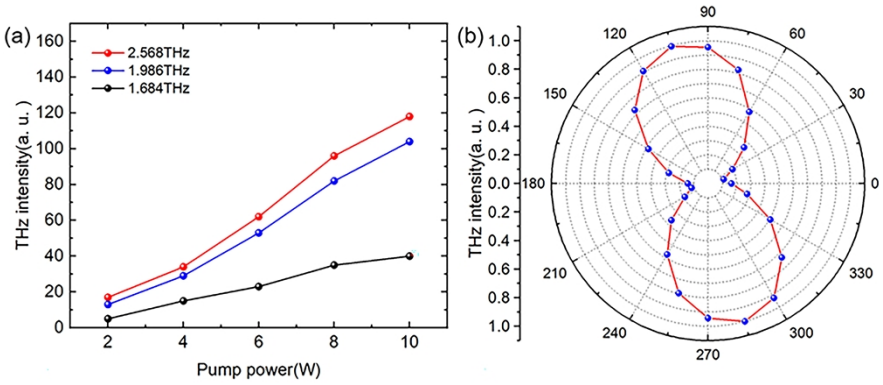

Fig. 3. (a) The dependence of the THz wave intensity and the pump power at 1.684THz, 1.986THz and 2.568THz. (b) Polarization characteristics of the THz wave at 2.568THz.

improvements in crystal growth and processing can lead to further improvement in THz-wave beam quality.

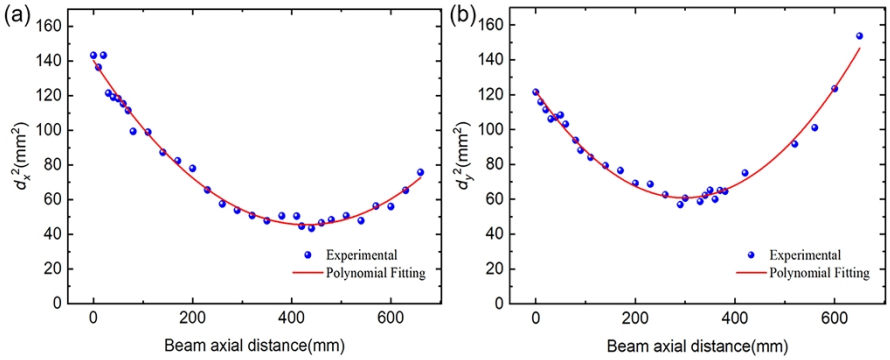

Fig. 4. The spatial distribution of the THz wave in (a) horizontal direction and (b) vertical direction at 2.568THz.

In order to figure out the linewidth of the CW-THz source, transmission spectra of lower pressure gas were investigated using a 25 cm long vacuum gas cell. Considering the spectra of carbon monoxide (CO) has several absorption lines in 1-3 THz range, it was used as the sample gas in this experiment. Moreover, the absorption line at 80.52 cm^{-1} was selected for detection, where both the absorption coefficient of CO and the intensity of THz signal were high. The absorption linewidth of CO is directly related to the gas pressure. Figure 5 shows the transmission spectra of CO gas around 2.4139 THz (80.52 cm^{-1}) at the pressure of 450 Pa. Assuming the THz wave had a Gaussian profile defined as $F(\lambda)$ and the low pressure gas absorption had a Lorentz profile defined as $G(\lambda)$ [27], the transmission spectra $H(\lambda)$ which had a Vogit profile was the convolution of the THz wave with the known CO gas absorption spectra (Hitran database), where it met $H(\lambda) = F(\lambda) * G(\lambda)$. The red line in Fig. 5 shows the fitted Vogit profile. The linewidth of CW-THz source can be estimated of 56.5 MHz using the empirical expression in Ref. [28]. It is worth mentioning that there was slight fluctuation in the measured data, which were mainly due to the wavelength drift of the pump lasers. When the absorption line is very narrow, the wavelength drift has a significant impact on the measured transmission spectra. The frequency feedback modules will be further added to get the actual linewidth of the THz wave under lower gas pressure.

Optics EXPRESS

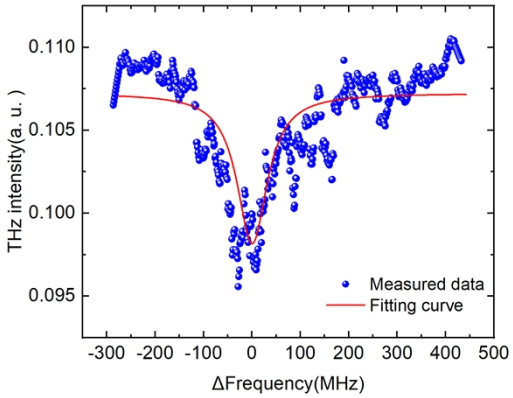

Fig. 5. Absorption spectrum of CO gas at 450 Pa.

Furthermore, the CW-THz output spectrum under the humidity of 40% was measured at room temperature, which was plotted by black color in Fig. 6(a). The path length from DAST crystal to the detection window of Bolometer was 5 cm. The THz transmittance spectra were measured in 124 MHz/step. For comparison, the air absorption line from Hitran database was also shown in Fig. 6(a) by red line. It can be seen from Fig. 6(a) that there are 23 output dips in 1.5-3.0THz (50-100 cm^{-1}) in THz output spectrum, corresponding to 53.45, 55.70, 57.27, 58.78, 59.92, 62.30, 64.02, 68.06, 69.19, 72.19, 73.26, 74.11, 75.53, 78.20, 78.92, 79.71, 82.16, 88.08, 88.88, 89.59, 92.53, 96.79 and 99.07 cm^{-1} in Hitran database. Especially, the positions of the THz output dips consisted well with the air absorption line. Table 1 gives the details of the measured and theoretical positions of these 23 absorption peaks, where the deviation between them was also listed. It can be seen that most of the deviations of the peak positions between measured and theoretical values were less than 500 MHz (about 4 scan steps). For most absorption lines, the reason for the deviations was mainly due to the wavelength drift during the tuning process of Laser1 (wavelength setting repeatability is 5 pm, corresponding to 600 MHz). For a few of weak absorption lines of water vapor (1.79627, 2.34426, 2.36594, 2.66459 and 2.68575 THz), low signal-to-noise ratio lead to relative larger deviations. Therefore, a frequency feedback module to the pump system is necessary to further improve the frequency stability and reduce these deviations. Furthermore, Fig. 6(b) shows the enlarged THz absorption spectra around the absorption peak at 1.67 THz. It can be seen that the absorption peak at 1.67 THz splits into two parts in Hitran database, where the left part has smaller absorption coefficient. Due to the narrow linewidth and high stability of the CW-THz source, the splitting phenomenon was also clearly displayed in the THz transmission spectra. Thus, the CW-THz source has the potential for high-precision spectroscopic detection.

Moreover, we measured the transmission spectra of 2-Deoxy-D-Glucose sample using the CW-THz source. The tablet mixed with high-density polyethylene (sigma-Aldrich, Shanghai, China) was prepared with the mixing ratio of 1:9. The mixture was grinded and then filtrated through a 200-mesh sieve to minimize the scattering effects from sample particles during spectral measurements. The mixed powder was pressed into circular tablets around 10 mm diameter and 2.0 mm thickness under 6 MPa pressure for 3 min. Five replicates of each sample were prepared for reproducibility assessment. Figure 7 shows the THz transmission spectrum of 2-deoxy-D-glucose tablets after S-G smoothing in the range of 1.50-2.85 THz. The fluctuations of the black line around 1.7 THz and 2.6-2.9 THz were due to water vapor absorption at 3% humidity in the measurement environment, which was similar to Fig. 2. It can be seen that the sample has three transmission dips at 1.88 THz, 2.13 THz and 2.41 THz, respectively. Here, full

Optics EXPRESS

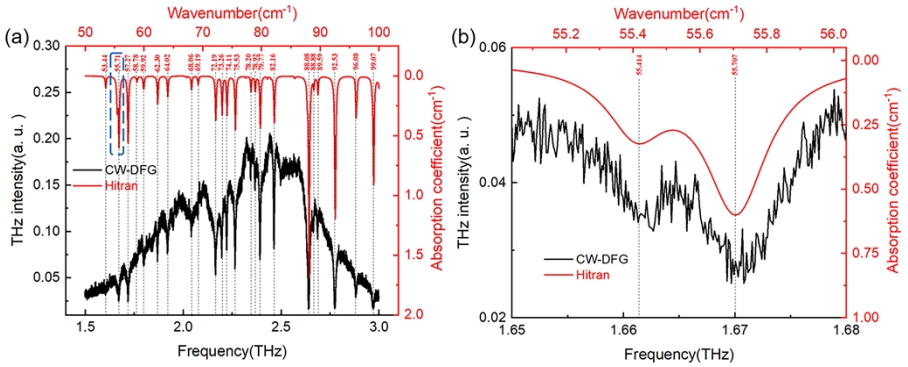

Fig. 6. Measured THz-wave intensity spectra at (a) 1.5-3.0 THz and (b) around 1.67 THz. Air absorption lines in Hitran database are shown with red lines.

Table 1. Measured and theoretical positions of air absorption peaks

Measured (THz)	Hitran database (THz)	Deviation (GHz)	Measured (THz)	Hitran database (THz)	Deviation (GHz)
1.60253	1.60242	0.11	2.26392	2.26424	-0.32
1.67023	1.67004	0.18	2.34473	2.34426	0.47
1.71681	1.71676	0.05	2.36628	2.36594	0.34
1.76238	1.76219	0.19	2.39155	2.39149	0.06
1.79684	1.79627	0.57	2.46297	2.46299	-0.02
1.86770	1.86777	-0.07	2.64012	2.64058	-0.46
1.91936	1.91938	-0.02	2.66358	2.66459	-1.01
2.04048	2.04045	0.03	2.68519	2.68575	-0.56
2.07428	2.07426	0.02	2.77416	2.77403	0.13
2.16443	2.16435	0.08	2.88066	2.88038	0.28
2.19608	2.19635	-0.27	2.97006	2.96994	0.12
2.22163	2.22165	-0.02			

width at half maximum (FWHM) was defined as the width at half the difference between the dip and the baseline, which was used to evaluate the width of the absorption peak. The FWHM of the dip at 1.88 THz were 82 GHz and 122 GHz from measurements using CW-THz source and RIKEN database, respectively. And the dips at 2.13 THz and 2.41THz were 57 GHz and 140 GHz using CW-THz source measurements, whereas the FWHM were 71 GHz and 144 GHz in RIKEN database, respectively. Thus, it is clear seen that the narrow linewidth THz wave can reflect the more detailed information of substances. It will facilitate the distinction between different substances of similar composition.

Optics EXPRESS

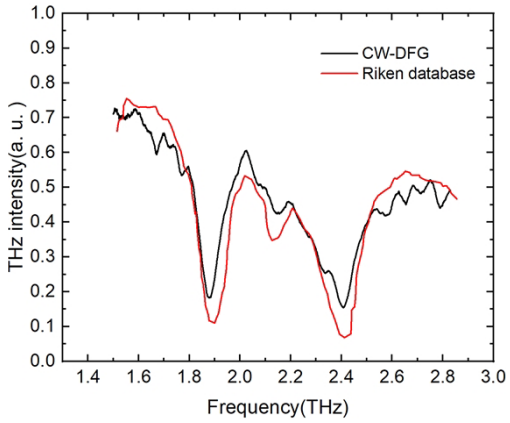

Fig. 7. THz transmittance spectra of 2-Deoxy-D-Glucose sample from CW-THz source (black line) and Riken Database (red line).

4. Conclusion

In conclusion, we have demonstrated a narrow linewidth, tunable CW THz source by DFG with DAST crystal. The THz wave was continuously tuned from 1.1 THz to 3 THz. The maximum output power was 2.79 nW at 2.568 THz, corresponding to the power conversion efficiency of 0.93×10^{-9}. The power fluctuation in 30 minutes was measured to be 2.41%. The linewidth of the output THz wave was estimated to be 56.5 MHz by fitting transmission spectrum of low pressures CO gas around 80.52 cm^{-1} using the Vogit gas model. Moreover, the output spectra at room temperature and pressure of the CW-THz source was in high agreement with the air absorption lines in Hitran database, which means it had high frequency resolution and stability. The spectral measurement of the 2-Deoxy-D-Glucose tablet showed that it is also applicable for high-precision spectral detection of solid samples. This CW-THz source is expected to be promising for high precision THz spectroscopic and imaging applications.

Funding. National Natural Science Foundation of China (62175182, 62275193, U22A20123, U22A20353).

Disclosures. The authors declare no conflicts of interest.

Data availability. Data underlying the results presented in this paper are not publicly available at this time but may be obtained from the authors upon reasonable request.

References

1. B. Ferguson and X. C. Zhang, "Materials for terahertz science and technology," Nat. Mater. **1**(1), 26–33 (2002).
2. C. Sirtori, "Applied physics: bridge for the terahertz gap," Nature **417**(6885), 132–133 (2002).
3. X. Yang, X. Zhao, K. Yang, *et al.*, "Biomedical Applications of Terahertz Spectroscopy and Imaging," Trends Biotechnol. **34**(10), 810–824 (2016).
4. L. A. Sterczewski, J. Westberg, Y. Yang, *et al.*, "Terahertz Spectroscopy of Gas Mixtures with Dual Quantum Cascade Laser Frequency Combs," ACS Photonics **7**(5), 1082–1087 (2020).
5. H. T. Stinson, A. Sternbach, O. Najera, *et al.*, "Imaging the nanoscale phase separation in vanadium dioxide thin films at terahertz frequencies," Nat. Commun. **9**(1), 3604 (2018).
6. M. Tonouchi, "Cutting-edge terahertz technology," Nat. Photonics **1**(2), 97–105 (2007).
7. L. S. Rothman, D. Jacquemart, A. Barbe, *et al.*, "The HITRAN 2004 molecular spectroscopic database," J. Quant. Spectrosc. Radiat. Transfer **96**(2), 139–204 (2005).
8. H. Aghasi, S. M. H. Naghavi, M. Tavakoli Taba, *et al.*, "Terahertz electronics: Application of wave propagation and nonlinear processes," Appl. Phys. Rev. **7**(2), 021302 (2020).
9. W. He, C. R. Donaldson, L. Zhang, *et al.*, "Broadband Amplification of Low-Terahertz Signals Using Axis-Encircling Electrons in a Helically Corrugated Interaction Region," Phys. Rev. Lett. **119**(18), 184801 (2017).
10. V. S. Cherkassky, B. A. Knyazev, V. V. Kubarev, *et al.*,. Vinokurov "Imaging techniques for a high-power THz free electron laser," *29th Infrared and Millimeter Waves*, (2004).

Optics EXPRESS

11. R. Chhantyal-Pun, A. Valavanis, J. T. Keeley, *et al.*, "Gas spectroscopy with integrated frequency monitoring through self-mixing in a terahertz quantum-cascade laser," Opt. Lett. **43**(10), 2225–2228 (2018).
12. E. R. Mueller, R. Henschke, W. E. Robotham, *et al.*, "Terahertz local oscillator for the microwave limb sounder on the aura satellite," Appl. Opt. **46**(22), 4907–4915 (2007).
13. S. Mansourzadeh, T. Vogel, M. Shalaby, *et al.*, "Milliwatt average power, MHz-repetition rate, broadband THz generation in organic crystal BNA with diamond substrate," Opt. Express **29**(24), 38946–38957 (2021).
14. K. Chen, L. Tang, D. Xu, *et al.*, "Continuously Tunable and Energy-Enhanced Injection Pulse-Seeded Terahertz Parametric Generator Based on KTP Crystal," ACS Photonics **8**(11), 3141–3149 (2021).
15. J. Nishizawa, T. Tanabe, K. Suto, *et al.*, "Continuous-Wave Frequency-Tunable Terahertz-Wave Generation From GaP," IEEE Photonics Technol. Lett. **18**(19), 2008–2010 (2006).
16. B. Dolasinski, P. E. Powers, J. W. Haus, *et al.*, "Tunable narrow band difference frequency THz wave generation in DAST via dual seed PPLN OPG," Opt. Express **23**(3), 3669–3680 (2015).
17. M. Tang, H. Minamide, Y. Wang, *et al.*, "Tunable Terahertz-wave generation from DAST crystal pumped by a monolithic dual-wavelength fiber laser," Opt. Express **19**(2), 779–786 (2011).
18. T. Tanabe, J.-i. Nishizawa, K. Suto, *et al.*, "Terahertz Wave Generation from GaP with Continuous Wave and Pulse Pumping in the 1-1.2 μm Region," Mater. Trans. **48**(5), 980–983 (2007).
19. P. D. Cunningham and L. M. Hayden, "Optical properties of DAST in the THz range," Opt. Express **18**(23), 23620–23625 (2010).
20. M. Jazbinsek, U. Puc, A. Abina, *et al.*, "Organic Crystals for THz Photonics," Appl. Sci. **9**(5), 882 (2019).
21. Y. He, Y. Wang, D. Xu, *et al.*, "High-energy and ultra-wideband tunable terahertz source with DAST crystal via difference frequency generation," Appl. Phys. B **124**, 16 (2017).
22. L. Cao, B. Teng, D. Xu, *et al.*, "Growth, transmission, Raman spectrum and THz generation of DAST crystal," RSC Adv. **6**(103), 101389 (2016).
23. J. R. Paul, M. Scheller, A. Laurain, *et al.*, "Narrow linewidth single-frequency terahertz source based on difference frequency generation of vertical-external-cavity source-emitting lasers in an external resonance cavity," Opt. Lett. **38**(18), 3654–3657 (2013).
24. T. A. G. Bondaz, A. Laurain, J. V. Moloney, *et al.*, "Generation and Stabilization of Continuous-Wave THz Emission From a Bi-Color VECSEL," IEEE Photonics Technol. Lett. **31**(19), 1569–1572 (2019).
25. M. Walther, K. Jensby, S. R. Keiding, *et al.*, "Far-infrared properties of DAST," Opt. Lett. **25**(12), 911–913 (2000).
26. H. Zhao, Y. Tan, T. Wu, *et al.*, "Efficient broadband terahertz generation from organic crystal BNA using near infrared pump," Appl. Phys. Lett. **114**(24), 241101 (2019).
27. D. Walsh, D. J. M. Stothard, T. J. Edwards, *et al.*, "Injection-seeded intracavity terahertz optical parametric oscillator," J. Opt. Soc. Am. B **26**(6), 1196–1202 (2009).
28. M. Chen, Z. Meng, J. Wang, *et al.*, "Ultra-narrow linewidth measurement based on Voigt profile fitting," Opt. Express **23**(5), 6803–6808 (2015).